

Approval Talk [HIG-23-005]

“Search for rare decays of the Higgs boson into a photon and a ρ^0 , ϕ or K^{*0} meson”

R. Covarelli^{1,2} M. Pelliccioni¹ G. Umoret^{1,2}
M. D'Alfonso³ G. Gomez Ceballos³ C. Paus³ K. Yoon³

¹INFN Torino, Turin, Italy

²Università degli Studi di Torino, Turin, Italy

³Massachusetts Institute of Technology, Cambridge, U.S.

March 19, 2024

Outline

About this analysis	3
Introduction	4
Analysis Strategy	7
Triggers	10
Simulated Samples	14
Event Selection	17
Multivariate Analysis Selection	23
Signal & Background Modeling	32
Systematic Uncertainties	35
Results	37
Backup Slides	49
References	54

HIG-23-005

Collaboration

- Collaboration of **MIT** and **Torino** groups, targeting different Higgs production categories.

Conveners

- **ARC**: Anadi Canepa (chair), Stefan Spanier, Jian Wang, Angelo Giacomo Zecchinelli
- **CCLE**: Christoph Maria Ernst Paus

Documentation

- Relevant links: [CADI](#), [TWiki](#), [Pre-Approval Talk](#), Unblinding Talk
- Latest ANs (two individual + one combined):
[AN-22-004](#) (MIT, v9), [AN-22-067](#) (Torino, v10), and [AN-23-004](#) (combined, v7)

Introduction

Higgs coupling with light quarks (u, d, s)

- Suppressed couplings and large QCD background hamper direct searches.
- Class of decays suggested $H \rightarrow M\gamma$, where M is a light-quark meson.
- *In this analysis, $M = \phi, \rho^0, K^{*0}$ are considered.*

Channel	Coupling	SM $\mathcal{BR}(H \rightarrow M\gamma)$
$H \rightarrow \phi\gamma$	s	$(1.68 \pm 0.08) \times 10^{-5}$ [1]
$H \rightarrow \rho^0\gamma$	u, d	$(2.31 \pm 0.11) \times 10^{-6}$ [1]
$H \rightarrow K^{*0}\gamma$	$d\&s$ (flavor-changing)	(Only available for $H \rightarrow d\bar{s} + \bar{d}s$) 1.19×10^{-11} [2]

Table 1: $H \rightarrow M\gamma$ channels considered in this analysis with their respective couplings and predicted branching ratios.

Motivations

$H \rightarrow M\gamma$

1. Flavor-conserving probes

- **Direct contribution.** The Higgs couples via Yukawa coupling to the quarks, one of which radiates a photon.
- **Indirect contribution.** The off-shell γ^* or Z^* produced in $H \rightarrow \gamma\gamma, \gamma Z^*$ fragments into a meson.

Direct and indirect contributions interfere destructively. Due to light quark masses, direct contribution is smaller than indirect. *Direct contribution is sensitive to deviation from SM.* Branching ratios are typically $\mathcal{O}(10^{-5}-10^{-6})$.

- ϕ : s quark coupling (*diagrams above*)
- ρ^0 : u and d quark coupling

2. Flavor-changing probe

- K^{*0} : flavor-changing s and d quarks via weak interaction (*diagrams below*)

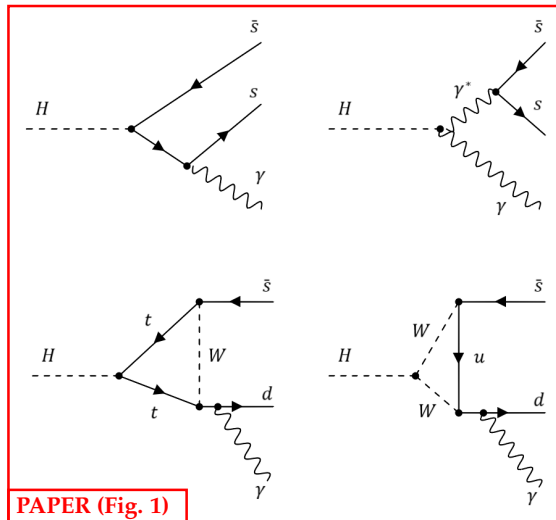


Figure 1: Feynman diagrams showing the different Higgs boson decay mechanisms into a photon and a light meson (top: ϕ meson; bottom: K^{*0} meson).

Analysis Strategy

Analysis Strategy

- **Final states**

1. High energy **photon**.
2. High energy **di-track** from meson.



$$\mathcal{BR}(\rho^0 \rightarrow \pi^+ \pi^-) \sim 100\%$$



$$\mathcal{BR}(\phi \rightarrow K^+ K^-) \sim 49\%$$



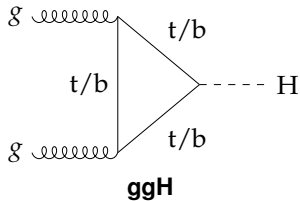
$$\mathcal{BR}(K^{*0} \rightarrow K^\pm \pi^\mp) \sim 100\%$$

Figure 2: Di-track systems for the different mesons considered in this analysis.

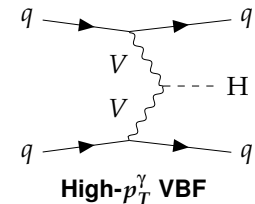
3. Signal events extracted from **photon & di-track invariant mass spectrum**.

Analysis Strategy

- **Higgs Production Categories**



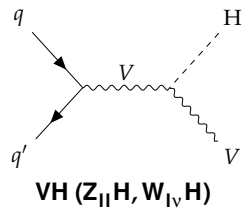
- No e/μ .



- $p_T^\gamma > 75 \text{ GeV}$.
- No e/μ

Low- p_T^γ VBF

- $38 < p_T^\gamma < 75 \text{ GeV}$.
- No e/μ



- At least one e/μ .
- Also included is $t\bar{t}H$, accounting for $\sim 30\%$.

Triggers

Triggers

- **High Level Triggers (HLT)**

Three types of triggers are employed.

Tau-like trigger

Photon + jets with τ -ID → ggH, low- p_T^γ VBF

- Photon $p_T^\gamma > 35$ GeV + tau-like jet $p_T^j > 35$ GeV.
- Tau-leg similar to isolated di-track system.
- Luminosity:
 39.50 fb^{-1} (2018).

VBF-dedicated trigger

High- p_T^γ photon + VBF-like jets → high- p_T^γ VBF

- Photon $p_T^\gamma > 75$ GeV + di-jet with large M_{jj} and $\Delta\eta_{jj}$.
- Active partly during 2016-17 and fully during 2018.
- Luminosities:
 28.2 fb^{-1} (2016), 7.7 fb^{-1} (2017), 60 fb^{-1} (2018).

Leptonic trigger

Double or single lepton → VH

- Single or double-muon (electron) lowest p_T thresholds vary depending on year.
- To complement selection, triggers requiring a lepton and a photon is also used.
- Luminosity:
 138 fb^{-1} (2018).

- **HLT Efficiencies and Scale Factors**

Trigger efficiency **scale factor** defined as the ratio of data vs. MC efficiency.

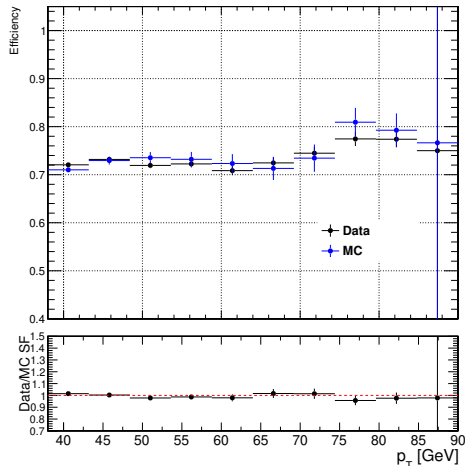
$$SF = \frac{\epsilon_{\text{Data}}}{\epsilon_{\text{MC}}}$$

- For the tau-like trigger, Data = Single Muon, MC = Drell-Yan.
Photon-leg and tau-leg efficiencies measured separately.
- Modification on photon-leg added to reduce fake photon rate by forcing the photon to be a FSR.

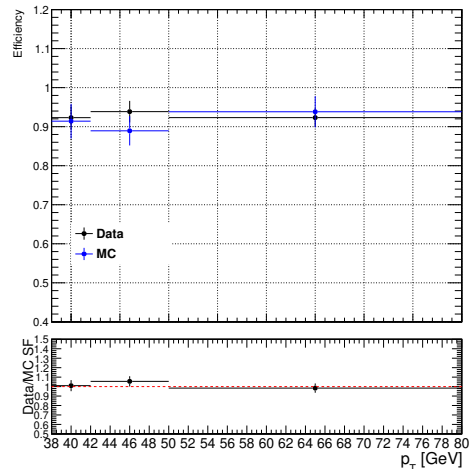
Triggers

- **HLT Efficiencies and Scale Factors**

Tau-like trigger efficiencies MC (blue) vs. Data (black).



(a) Tau-like trigger photon-leg efficiencies for MC and data.



(b) Tau-like trigger tau-leg efficiencies for MC and data.

Figure 3: Photon-leg and tau-leg efficiencies of the tau-like trigger.

Simulated Samples

Simulated Samples

- **MC Generation**

Gen-level: POWHEG (NLO) or MADGRAPH5_aMC@NLC (LO)

PDFs: NNPDF3.1 (NNLO)

Hadronization: PYTHIA 8.212

- SM processes considered in background simulation are γ , $W \rightarrow l\nu$, Drell-Yan $Z \rightarrow ll$ with jets, $t\bar{t}$, $W\gamma$, and $Z\gamma$.
- Cross sections for Higgs production:

Process	σ (fb)
ggH	48580
VBF	3782
$W_{l\nu}H$	471
$Z_{ll}H$	77
$ggZ_{ll}H$	12

Simulated Samples

- **Signal Simulation**

Polarization reweighting of events.

Higgs is a scalar, and angular momentum conservation constrains the mesons to have transverse spin alignment in the $H \rightarrow M\gamma$ process. PYTHIA simulates unpolarized decay products. Therefore, signal events are reweighted by $(3/2) \sin^2 \theta$, where θ is the angle between positive track in meson rest frame and meson flight direction in lab frame.

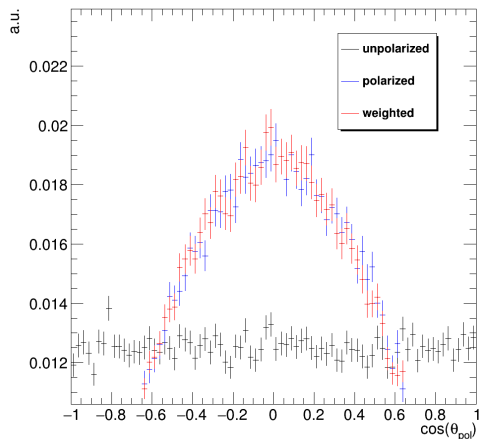


Figure 4: $\cos \theta$ for the ρ meson decay. The black flat distribution illustrates the polarization angle within the centrally produced MC signal. The blue distribution portrays a privately generated MC signal wherein the accurate polarization was already incorporated. The red distribution results from reweighting the black distribution using the reweighting technique outlined in this section.

Event Selection

Event Selection

- **Photon selection**

	ggH	High-p_T^γ VBF	Low-p_T^γ VBF	VH
p_T^γ [GeV]	> 38	> 75	$38 < p_T^\gamma < 75$	> 40
$ \eta^\gamma $	< 2.1	< 1.4	< 2.1	< 2.5
γ -ID signal eff.	80%	90%	80%	90%

Table 2: Photon selection criteria across different production categories.

- γ -ID signal eff. = MVA-based selection ID [3]
- p_T^γ and $|\eta^\gamma|$ cuts based on trigger thresholds and barrel vs. endcap considerations.
- ggH/VBF: conversion veto, VH: pixel veto.
- Highest- p_T^γ photon chosen as candidate.

- **Di-track system reconstruction**

Track selection

- Originate from PV.
- Pass “high purity” criteria.

Meson definition

- Pair of oppositely charged tracks.
- $p_T > 5 \text{ GeV}$, $|\eta| < 2.5$.
- At least one track $p_T > 20 \text{ GeV}$.

Invariant mass

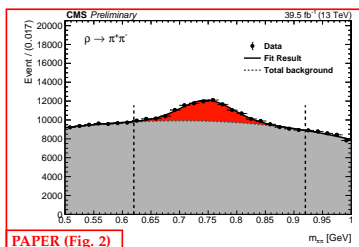
- Di-track system invariant **mass windows and sidebands** (next slide).
- $K^\pm\pi^\mp$ system: if both combinations exist, then the one closest to $m_{K^{*0}}$ is selected.
- Reject events where m_{KK} consistent with $m_{\pi\pi}/m_{K\pi}$ and have higher p_T , vice versa.

Applies to all production categories.

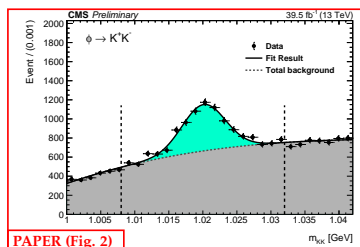
Event Selection

- **Di-track system reconstruction**

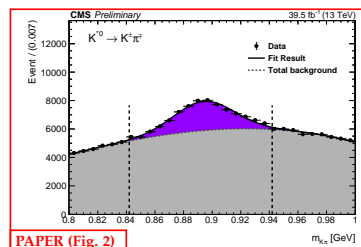
Mass windows applied to invariant mass of di-track system.



ρ^0 mass window: $0.62 < m_{\pi\pi} < 0.92$ GeV
Sidebands: $0.50 < m_{\pi\pi} < 0.62$ GeV
 $0.92 < m_{\pi\pi} < 1.00$ GeV



ϕ mass window: $1.008 < m_{KK} < 1.032$ GeV
Sidebands: $1.000 < m_{KK} < 1.008$ GeV
 $1.032 < m_{KK} < 1.042$ GeV



K^{*0} mass window: $0.84 < m_{K\pi} < 0.94$ GeV
Sidebands: $0.80 < m_{K\pi} < 0.84$ GeV
 $0.94 < m_{K\pi} < 1.00$ GeV

Figure 5: Di-track mass distribution in selected events in data, for the ggH category of the analysis, $\rho^0\gamma$ (left), $\phi\gamma$ (middle) and $K^{*0}\gamma$ (right) channels. Vertical dashed lines represent the signal mass region borders.

For more information on meson mass resolution, see backup slide 53.

Event Selection

- **Di-track system selection**

Define the relative **charged isolation** of the leading meson candidate,

$$I^{\text{trk}}(M) = \frac{p_T^M}{p_T^M + \sum_{\text{trk}} |p_T^{\text{trk}}|},$$

and the **neutral isolation** as

$$I^{\text{neu}}(M) = \frac{p_T^M}{p_T^M + \sum_{\text{neu}} |p_T^{\text{neu}}|}.$$

$\sum_{\text{trk/neu}} |p_T^{\text{trk/neu}}|$: sum of charged/neutral track p_T within $\Delta R = 0.3$ of meson candidate.

	ggH	High- p_T^γ VBF	Low- p_T^γ VBF	VH
p_T^M [GeV]	> 38	> 30	> 38	> 38
I_M^{trk}	> 0.9	> 0.9	> 0.9	> 0.8
I_M^{neu}	> 0.8	-	-	-

Table 3: Di-track system criteria across different production categories.

Event Selection

- Event tagging

	ggH	High- p_T^γ VBF	Low- p_T^γ VBF	VH
Event tagging	Meson candidate within a jet with $p_T^j > 40$ GeV, tracks with $\Delta R < 0.07$	2 jets with $p_T^j > 40$ GeV, $m_{jj} > 400$ GeV, $\eta_{jj} > 3$	2 jets with $p_T^j > 30, 20$ GeV, $m_{jj} > 300$ GeV, $\eta_{jj} > 3$	1 selected and isolated e/μ or 2 selected e/μ compatible with m_Z

Table 4: Event tagging selection criteria across different production categories.

Multivariate Analysis Selection

- **Multivariate Analysis (MVA) Overview**

Motivation

Improvement of signal-to-background ratio in categories with backgrounds dominated by $\gamma + \text{jet}$ and multijet events. → **ggH, low- p_T^γ VBF**, and **high- p_T^γ VBF** categories.

Methodology

- BDT classifiers based on ROOT TMVA [4], optimized with the Gradient boosting method.
- Training and validation samples defined by **meson mass SR & sidebands**.
- Signal & Background events weighted by $1/(\sigma M/M)$, where

$$\frac{\sigma M}{M} = \sqrt{\left(\frac{\sigma M}{M}\right)_{\text{meson}}^2 + \left(\frac{\sigma E}{E}\right)_\gamma^2}$$

- BDT classification is further split into **two sub-categories** (“cat0” and “cat1”) based on optimized discriminator threshold values to improve upper limit results.

Multivariate Analysis Selection

- MVA Overview

Input variables:

	ggH	High- p_T^γ VBF	Low- p_T^γ VBF
Kinematics	p_T^γ	$p_T^{M\gamma}$	$p_T^{M\gamma}$
	p_T^M	p_T^γ	p_T^γ
	η_M	$p_T^M/m_{M\gamma}$	$p_T^M/m_{M\gamma}$
Charged Isolation	$I^{\text{trk}}(\text{trk}_1)$	$I^{\text{trk}}(M)$	$I^{\text{trk}}(M)$
Photon ID		γ mvaID	γ mvaID
Jet-related		M_{jj}	M_{jj}
		$\Delta\phi_{jj}$	$\Delta\phi_{jj}$
		z^*	z^*

Table 5: Input variables used for ggH and VBF categories.

z^* is the Zeppenfeld variable, defined as $z^* = |\eta_{M\gamma} - 0.5(\eta_{j1} + \eta_{j2})| / |\Delta\eta_{jj}|$.

Multivariate Analysis Selection

- MVA: ggH category

- Training samples

Signal: MC-generated.

Background: Data from meson mass sidebands.

- 4 input variables

p_T^γ	photon p_T
p_T^M	meson p_T
η_M	meson η
$I^{\text{trk}}(\text{trk}_1)$	leading-track charged isolation

- BDT sub-categories

cat0: BDT-score > 0.55, optimized for max value of S/\sqrt{B} .

cat1: $-0.4 < \text{BDT-score} < 0.55$

Multivariate Analysis Selection

- MVA: ggH category

- Training results:

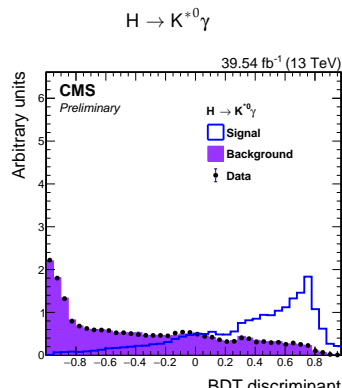
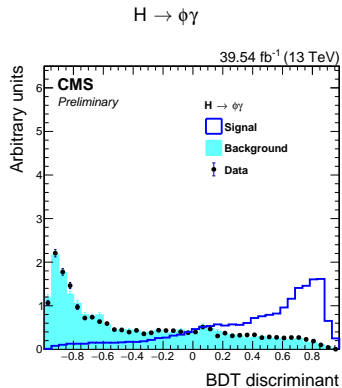
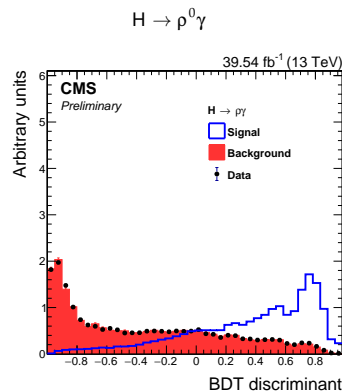


Figure 6: BDT-score shown for the three decay channels of ggH.

Multivariate Analysis Selection

- **MVA: High & Low- p_T^γ VBF categories**

- Training samples

Signal: MC-generated.

Background: γ +jets simulation and γ di-track events where the two tracks have the same charge.

- 8 input variables

Variable that is correlated with Higgs candidate mass is divided by the mass.

$p_T^{M\gamma}$	Higgs candidate p_T
p_T^γ	photon p_T
$p_T^M / m_{M\gamma}$	meson p_T divided by Higgs candidate mass
$I^{\text{trk}}(M)$	meson charged isolation
γ mvalID	photon identification discriminator
M_{jj}	di-jet invariant mass
$\Delta\phi_{jj}$	$\Delta\phi$ of the two jets
z^*	Zeppenfeld variable

- BDT sub-categories

cat0: BDT-score > 0.7 , optimized for max value of S/\sqrt{B} .

cat1: $-0.6 < \text{BDT-score} < 0.7$

Multivariate Analysis Selection

- **MVA: High- p_T^γ category**

- Training results:

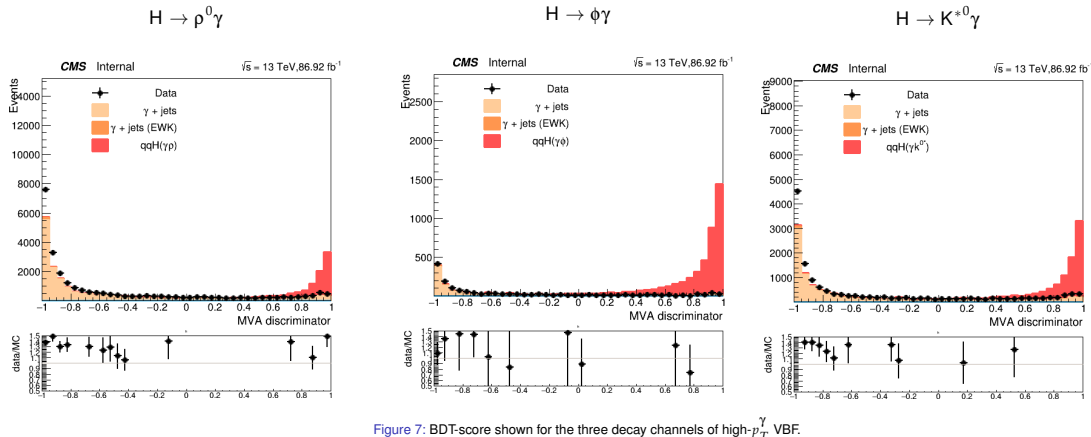
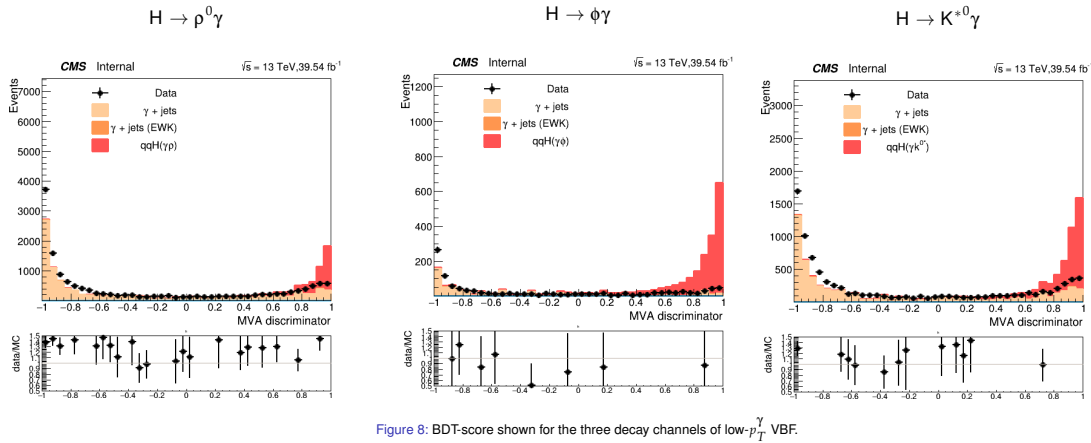


Figure 7: BDT-score shown for the three decay channels of high- p_T^γ VBF.

Multivariate Analysis Selection

- **MVA: Low- p_T^γ category**

- Training results:



Event Selection

Summary of Event Selection

Common selections				
2 "high-purity" tracks, opposite sign				
$ \eta^{\text{trk}} < 2.5, p_T^{\text{trk}1} > 20 \text{ GeV}, p_T^{\text{trk}2} > 5 \text{ GeV}, \eta^M < 2.1$				
M selection	$0.62 < m_{\pi\pi} < 0.92 \text{ GeV} (\rho^0) / 1.008 < m_{KK} < 1.032 \text{ GeV} (\phi) / 0.84 < m_{K\pi} < 0.94 \text{ GeV} (K^{*0})$			
Category	ggH	VBF high- p_T^γ	VBF low- p_T^γ	VH
Trigger	Photon + jet with τ -ID	high- p_T photon + VBF-like jets	Photon + jet with τ -ID	Double or single lepton
p_T^γ [GeV]	> 38	> 75	> 38 and < 75	> 40
$ \eta^\gamma $	< 2.5	< 1.4	< 2.1	< 2.5
γ -ID signal eff.	80%	90%	80%	90%
p_T^M [GeV]	> 38	> 30	> 38	> 38
$I^{\text{trk}}(M)$	> 0.9	> 0.9	> 0.9	> 0.8
$I^{\text{neu}}(M)$	> 0.8	-	-	-
Event tagging	Meson candidate within a jet with $p_T^j > 40$ GeV, tracks with $\Delta R < 0.07$	2 jets with $p_T^j > 40$ GeV	2 jets with $p_T^j > 30/20$ GeV	1 selected and isolated e/ μ or 2 selected e/ μ compatible with Z mass
BDT categories				
cat0	BDT > 0.55	BDT > 0.7	BDT > 0.7	-
cat1	$-0.4 < \text{BDT} < 0.55$	$-0.6 < \text{BDT} < 0.7$	$-0.6 < \text{BDT} < 0.7$	-
PAPER (Table 1)				

Figure 9: Summary of the event selections, including both common and category-specific selections.

Signal & Background Modeling

Signal modeling

- Signal events extracted from the distribution of the **reconstructed Higgs boson mass**.
- Analytic function: **two-tailed Crystal Ball(TTCB)**.

$$\text{TTCB}(t) = \begin{cases} e^{-t^2/2}, & \text{for } -\alpha_L < t < \alpha_R \\ (\frac{n_L}{|\alpha_L|})^{n_L} e^{-\alpha_L^2/2} (\frac{n_L}{|\alpha_L|} - |\alpha_L| - t)^{-n_L}, & \text{for } t \leq -\alpha_L \\ (\frac{n_R}{|\alpha_R|})^{n_R} e^{-\alpha_R^2/2} (\frac{n_R}{|\alpha_R|} - |\alpha_R| + t)^{-n_R}, & \text{for } t \geq \alpha_L \end{cases}$$

- Fitted via unbinned likelihood to simulated signal events.

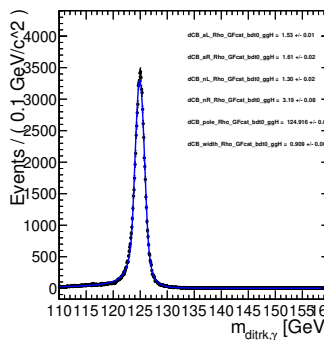


Figure 10: Example fitting of the TTCB function to the $H \rightarrow \rho^0 \gamma$ selected signal samples from BDT cat0 in the ggH category.

- Analytic functions: **Chebychev** polynomials (main), **Bernstein** polynomials and **exponential** series (determination of shape uncertainties).
- Fitting region defined as $m_{M\gamma}$ sidebands.
 - ggH category: $110 < m_{M\gamma} < 120$ GeV & $130 < m_{M\gamma} < 160$ GeV.
 - VBF categories (high & low p_T^γ): $100 < m_{M\gamma} < 120$ GeV & $130 < m_{M\gamma} < 170$ GeV.
 - VH category: $100 < m_{M\gamma} < 120$ GeV & $130 < m_{M\gamma} < 150$ GeV.
- Degree of polynomial determined with **F-test**.
- **Bias studies** performed.

Systematic Uncertainties

Systematic Uncertainties

Signal uncertainty

Integrated Luminosity	2.5% (2016), 2.3% (2017), and 2.5% (2018)
Total inelastic cross section	4.6%
Trigger efficiencies	VBF-dedicated trigger, 2.2-3.4% (photon-leg) and 5.3-5.6% (di-jet)
Photon ID efficiencies	Up to 1.5%, p_T and η dependent
Tracking efficiency	4.6% (2.3% per track)
Muon/Electron ID	Less than 1.0% (muons) / 1.5% (electrons)
Meson Charged/Neutral Isolation Efficiencies	1.7-2.8 %, depending on search channel and isolation type
JEC & JES	Up to 3.5% in VBF, negligible in ggH
QCD renormalization and factorization	0.4% (VBF), 0.7% (WH), 3.8% (ZH), and 2.6% ($t\bar{t}H$)
PDF & α_S	1.6-3.2%, depending on Higgs production
Parton shower modeling	$\mathcal{O}(0.1\%)$

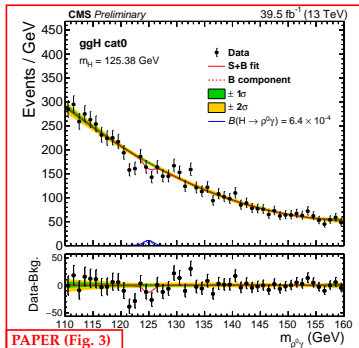
Table 6: Table of systematic uncertainties.

Background shape uncertainty measured via **discrete profiling method**.

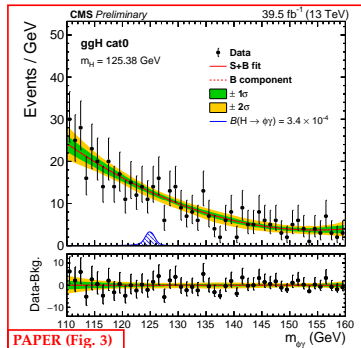
Results

Signal & Background Post-fit Distributions

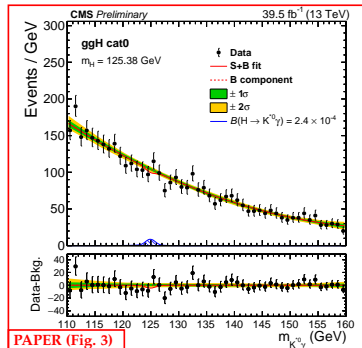
- ggH categories



$H \rightarrow \rho^0\gamma$, ggH cat0



$H \rightarrow \phi\gamma$, ggH cat0

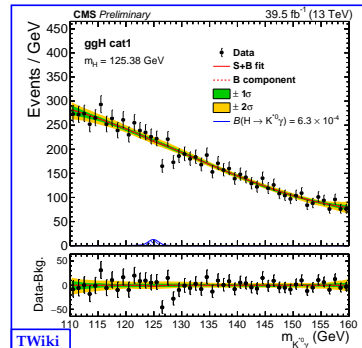
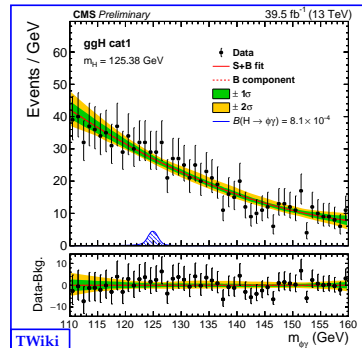
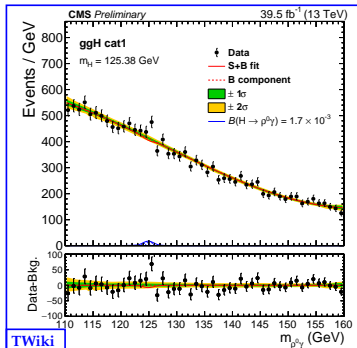


$H \rightarrow K^{*0}\gamma$, ggH cat0

Figure 11: Post-fit $m_{M\gamma}$ distributions in data and the background model for the ggH cat0 channels.

Signal & Background Post-fit Distributions

- ggH categories



$H \rightarrow \rho^0 \gamma$, ggH cat1

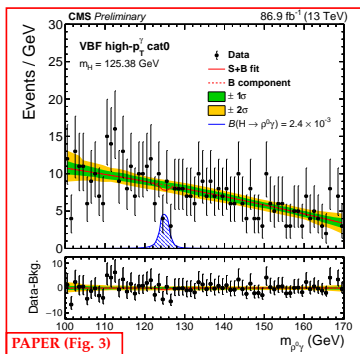
$H \rightarrow \phi \gamma$, ggH cat1

$H \rightarrow K^0 \gamma$, ggH cat1

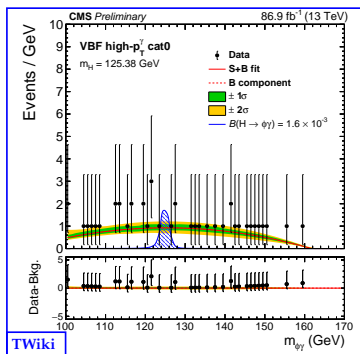
Figure 12: Post-fit $m_{M\gamma}$ distributions in data and the background model for the ggH cat1 channels.

Signal & Background Post-fit Distributions

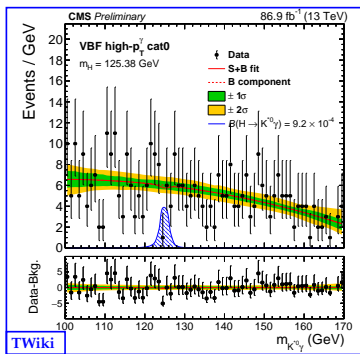
- High- p_T^γ VBF categories



$H \rightarrow p^0\gamma$, high- p_T^γ VBF cat0



$H \rightarrow \phi\gamma$, high- p_T^γ VBF cat0

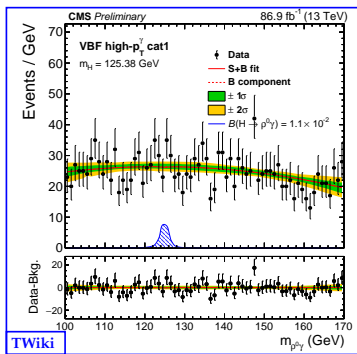


$H \rightarrow K^{*0}\gamma$, high- p_T^γ VBF cat0

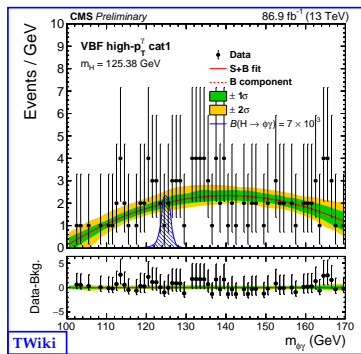
Figure 13: Post-fit $m_{M\gamma}$ distributions in data and the background model for the high- p_T^γ VBF cat0 channels.

Signal & Background Post-fit Distributions

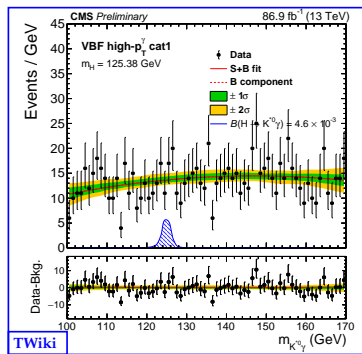
- High- p_T^γ VBF categories



$H \rightarrow \rho^0 \gamma$, high- p_T^γ VBF cat1



$H \rightarrow \phi \gamma$, high- p_T^γ VBF cat1

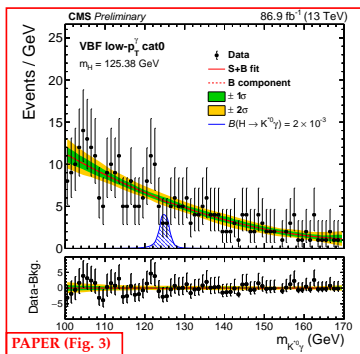


$H \rightarrow K^{*0} \gamma$, high- p_T^γ VBF cat1

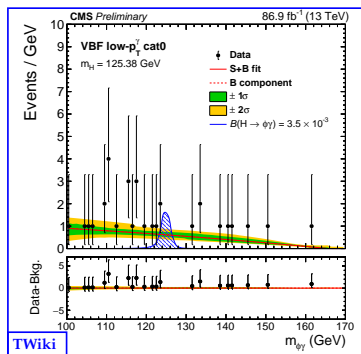
Figure 14: Post-fit m_{M_Y} distributions in data and the background model for the high- p_T^γ cat1 channels.

Signal & Background Post-fit Distributions

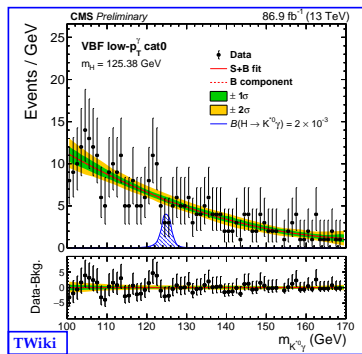
- Low- p_T^γ VBF categories



$H \rightarrow p^0 \gamma$, low- p_T^γ VBF cat0



$H \rightarrow \phi \gamma$, low- p_T^γ VBF cat0

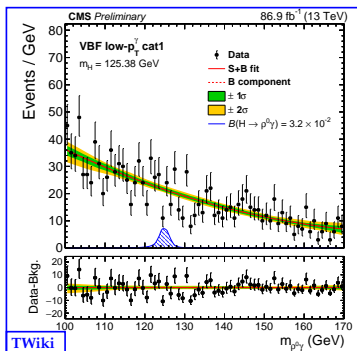


$H \rightarrow K^{*0} \gamma$, low- p_T^γ VBF cat0

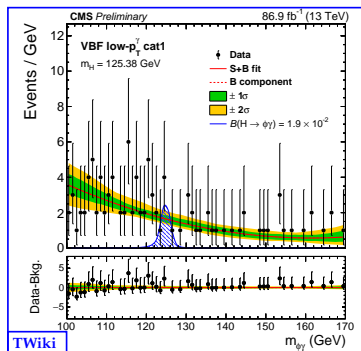
Figure 15: Post-fit $m_{M\gamma}$ distributions in data and the background model for the low- p_T^γ VBF cat0 channels.

Signal & Background Post-fit Distributions

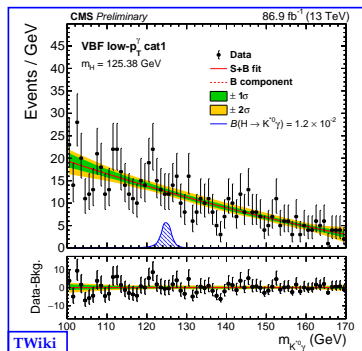
- Low- p_T^γ VBF categories



$H \rightarrow p^0\gamma$, low- p_T^γ VBF cat1



$H \rightarrow \phi\gamma$, low- p_T^γ VBF cat1

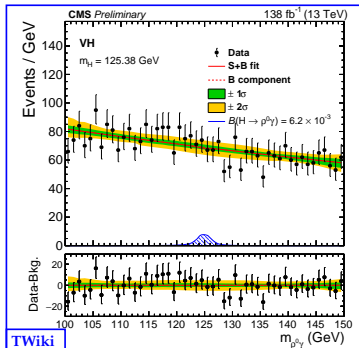


$H \rightarrow K^{*0}\gamma$, low- p_T^γ VBF cat1

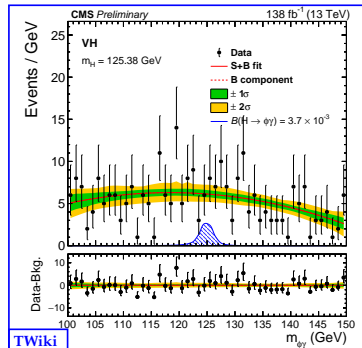
Figure 16: Post-fit m_{M_γ} distributions in data and the background model for the low- p_T^γ cat1 channels.

Signal & Background Post-fit Distributions

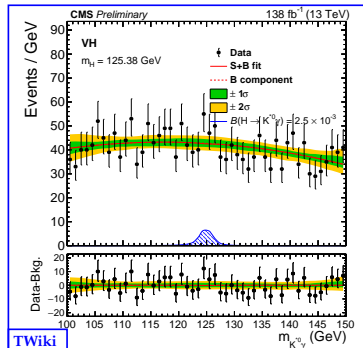
- VH categories



$H \rightarrow p^0\gamma, \text{VH}$



$H \rightarrow \phi\gamma, \text{VH}$



$H \rightarrow K^{*0}\gamma, \text{VH}$

Figure 17: Post-fit m_{M_Y} distributions in data and the background model for the VH channels.

Upper Limits

- **Upper limits** on $\mathcal{B}(H \rightarrow \rho^0\gamma)$, $\mathcal{B}(H \rightarrow \phi\gamma)$, and $\mathcal{B}(H \rightarrow K^{*0}\gamma)$ set at 95% CL.
- CLs profile-likelihood ratio used as test-statistics, with the asymptotic approximation.
- Systematic uncertainties treated as nuisance parameters.

Upper Limits

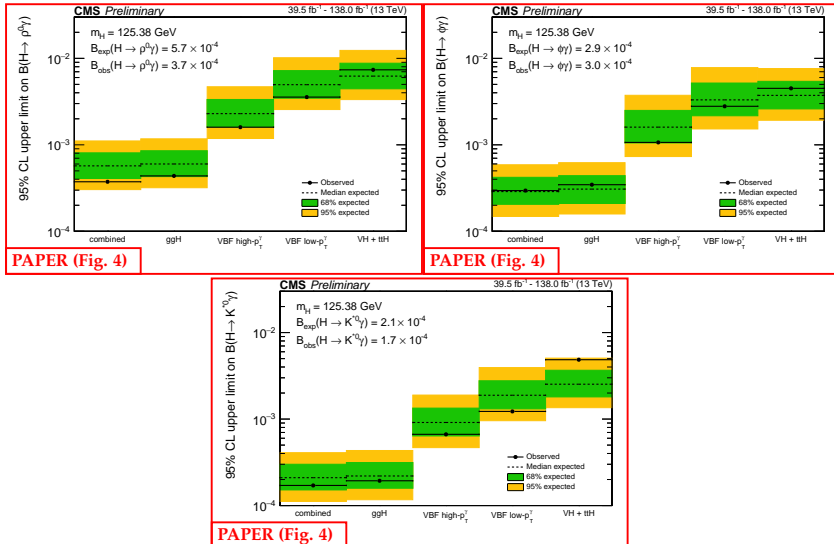


Figure 18: Expected and observed upper limits on $B(H \rightarrow \rho^0\gamma)$ (top left), $B(H \rightarrow \phi\gamma)$ (top right), and $B(H \rightarrow K_0^*\gamma)$ (bottom) split by analysis categories and combined. Green and yellow bands correspond to 1 and 2σ confidence intervals in the expected upper limits.

Results

	U.L. $\mathcal{B}(H \rightarrow \rho^0 \gamma)$		U.L. $\mathcal{B}(H \rightarrow \phi \gamma)$		U.L. $\mathcal{B}(H \rightarrow K^{*0} \gamma)$	
category	Exp. (10^{-4})	Obs. (10^{-4})	Exp. (10^{-4})	Obs. (10^{-4})	Exp. (10^{-4})	Obs. (10^{-4})
VH	$62.3^{+25.6}_{-17.9}$	73.7	$37.3^{+16.9}_{-11.3}$	45.0	$25.3^{+11.4}_{-7.3}$	48.5
low- p_T^γ VBF	$49.6^{+22.5}_{-15.0}$	35.6	$33.1^{+18.7}_{-11.5}$	27.9	$18.8^{+8.90}_{-5.7}$	12.3
high- p_T^γ VBF	$22.9^{+10.5}_{-6.9}$	16.0	$16.0^{+9.0}_{-5.5}$	10.7	$9.13^{+4.25}_{-2.75}$	6.66
ggH	$6.01^{+2.53}_{-1.72}$	4.37	$3.08^{+1.33}_{-0.98}$	3.46	$2.20^{+0.94}_{-0.62}$	1.93
combined	$5.71^{+2.37}_{-1.63}$	3.74	$2.88^{+1.33}_{-0.83}$	2.97	$2.10^{+0.90}_{-0.58}$	1.71

PAPER (Table 2)

Figure 19: Exclusion limits at 95% CL on the branching fractions of the H boson decays. Observed and median expected limits with the upper and lower bounds in the expected 68% CL intervals are reported.

Results Comparison

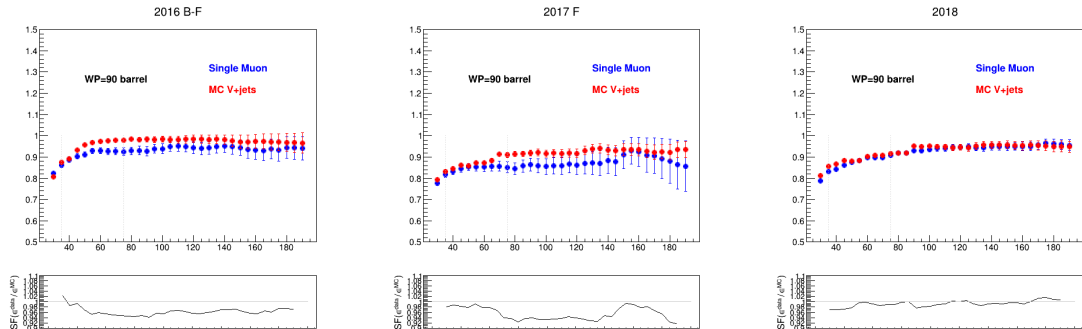
Channel	Coupling	SM $\mathcal{BR}(H \rightarrow M\gamma)$	ATLAS Limits (10^{-4})	Our Limits (10^{-4})
$H \rightarrow \rho^0 \gamma$	u, d	$(2.31 \pm 0.11) \times 10^{-6}$ [1]	Exp. $10.0^{+4.9}_{-2.8}$ Obs. 10.4 [5]	Exp. $5.71^{+2.37}_{-1.63}$ Obs. 3.74
$H \rightarrow \phi \gamma$	s	$(1.68 \pm 0.08) \times 10^{-5}$ [1]	Exp. $4.2^{+1.8}_{-1.2}$ Obs. 5.0 [5]	Exp. $2.88^{+1.33}_{-0.83}$ Obs. 2.97
$H \rightarrow K^{*0} \gamma$	$d\&s$ (flavor-changing)	(Only available for $H \rightarrow d\bar{s} + \bar{d}s$) 1.19×10^{-11} [2]	Exp. $3.7^{+1.5}_{-1.0}$ Obs. 2.2 [6]	Exp. $2.10^{+0.90}_{-0.58}$ Obs. 1.71

Table 7: Comparison of branching ratios obtained from theory, ATLAS, and this analysis.

Backup Slides

VBF Triggers

- VBF-dedicated trigger efficiencies MC (red) vs. Data (blue).



(a) VBF trigger photon-leg efficiencies for MC and data.

Figure 20: VBF-dedicated trigger photon-leg efficiencies for MC and data, shown for the $H \rightarrow p^0 \gamma$ channel in 2016 (top-left), 2017 (top-right), and 2018 (bottom).

Di-track Isolation Scale Factors

This slide was presented during the unblinding talk.

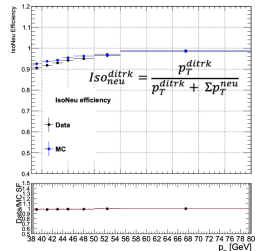
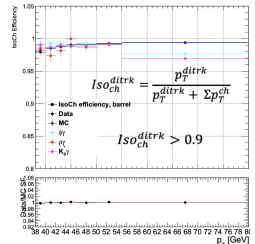
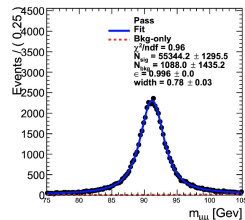
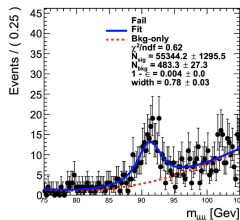


Di-track isolation efficiency

- Strategy: $Z \rightarrow \mu\mu$ T&P
- probe μ used as a proxy of di-track candidate
- Efficiencies calculated for Iso_{ch}^{ditrk} and Iso_{neu}^{ditrk}

More details:

- tag μ : must fire the IsoMu HLT, medium muonID, medium relative isolation wp
- probe μ : no stringent requirements, no isolation requirements
- $p_T^{\mu_{probe}}$ binned scale factors
- simultaneous fit to the dimuon mass in pass and fail region
- simFit example for the last MC bin



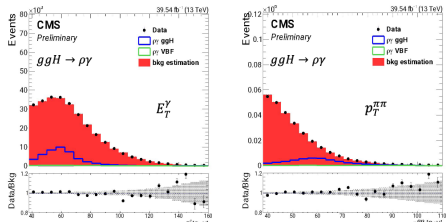
Background Estimation ggG

This slide was presented during the unblinding talk.

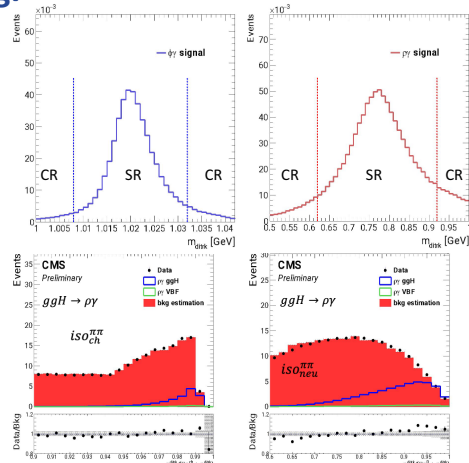


Background estimation ggF

- **Data driven bkg estimation** exploiting meson narrow peak
- Sidebands of ditrack invariant mass:
 $m_{\pi\pi} < 0.62 \text{ GeV} \parallel m_{\pi\pi} > 0.92 \text{ GeV}$
 $m_{KK} < 1.008 \text{ GeV} \parallel m_{KK} > 1.032 \text{ GeV}$
- bkg estimation from events in m_{ditrk} sidebands normalized to SR events



HIG-23-005 Unblinding Talk, Dec 19th – Giulio Umoret



Meson Mass Resolution

Meson	Resolution from $m_{\text{ditrk}}^{\text{reco}} - m_{\text{ditrk}}^{\text{gen}}$ fit (MeV)	Width from $m_{\text{ditrk}}^{\text{reco}}$ plot (MeV)	Width from PDG (MeV)
ρ^0	8.89	90	147
ϕ	2.22	6.4	4.25
K^{*0}	6.08	42	41

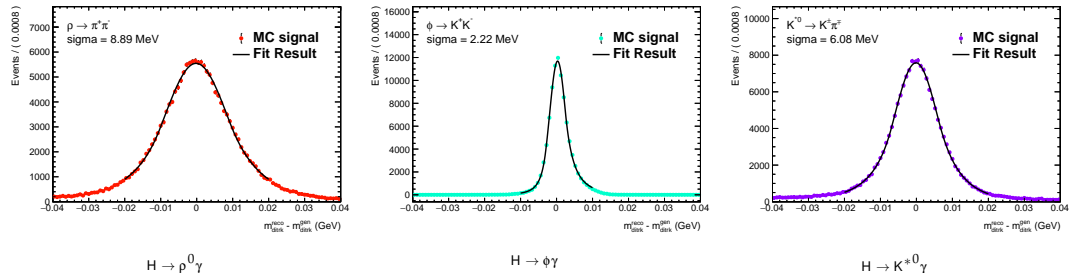


Figure 21: $m_{\text{ditrk}}^{\text{reco}} - m_{\text{ditrk}}^{\text{gen}}$ and Gaussian fit shown for the three decay channels.

References

- [1] M. König and M. Neubert, "Exclusive radiative Higgs decays as probes of light-quark Yukawa couplings", *Journal of High Energy Physics* **2015** (2015) .
- [2] J.I. Aranda, G. González-Estrada, J. Montaño et al., "Revisiting the rare $H \rightarrow q_i q_j$ decays in the standard model", *Journal of Physics G: Nuclear and Particle Physics* **47** (2020) 125001.
- [3] CMS collaboration, "Electron and photon reconstruction and identification with the CMS experiment at the CERN LHC", *Journal of Instrumentation* **16** (2021) P05014.
- [4] A. Hoecker, P. Speckmayer, J. Stelzer et al., "TMVA - Toolkit for Multivariate Data Analysis", 2009.
- [5] ATLAS collaboration, "Erratum to: Search for exclusive Higgs and Z boson decays to $\phi\gamma$ and $\rho\gamma$ with the ATLAS detector", *Journal of High Energy Physics* **2023** (2023) .
- [6] ATLAS collaboration, "Search for exclusive Higgs and Z boson decays to $\omega\gamma$ and Higgs boson decays to $K_0^*\gamma$ with the ATLAS detector", *Physics Letters B* **847** (2023) 138292.